Journal of Science and Education (JSE)
Vol 6, Issue 1, September 2025, Pages 878-890
ISSN: 2745-5351 (Media Online)
DOI: https://doi.org/10.58905/jse.v6i1.589

Design of a Mobile Carbon Monoxide (CO) Monitoring Device for Air Quality Mapping

Yogi Adi Nugraha*, Emir Husni, Galang Adira Prayoga

School of Electrical Engineering and Informatics, Institut Teknologi Bandung, Jl. Ganesha 10 Bandung 40132, Indonesia
Corresponding Email: yogi.adinugraha@gmail.com

Abstract. Air pollution monitoring in urban areas requires portable and real-time solutions to overcome the limitations of fixed monitoring stations. This study aims to design and develop a mobile carbon monoxide (CO) monitoring device to support urban air quality mapping. The proposed system integrates Internet of Things (IoT) technology, including the MiCS-4514 gas sensor, ESP32 microcontroller, Bluetooth, and Wi-Fi communication. Data transmission is conducted through the MQTT protocol to the Antares cloud platform. To ensure consistent measurement in motion, the device is equipped with a protective air chamber, DC pump, and flowmeter with a constant airflow of 1 liter per minute. Sensor calibration using the span gas method achieved a relative standard deviation of 1.58%, within the acceptable threshold and confirming valid precision. Field testing was conducted in two scenarios: static (indoor and outdoor) and mobile. Static tests demonstrated that sensor performance is highly influenced by wind direction and proximity to emission sources. Mobile tests were performed across three routes in Bandung City, covering a total of approximately 24 km during morning, midday, and evening periods. The average CO concentrations recorded were 3.76 ppm, 2.90 ppm, and 3.93 ppm, respectively. The highest detection rate, 7.8%, occurred during midday monitoring. The developed device successfully detected spatial CO distribution in real-time under dynamic conditions. This research contributes to the development of adaptive and efficient mobile air quality monitoring technologies, supporting data-driven environmental decision-making and potential integration with smart city systems.

Keywords: Air quality; Carbon monoxide; IoT; Mobile monitoring; Sensor system

1 Introduction

Urban areas in developing countries are increasingly facing environmental challenges due to rapid population growth and rising vehicle numbers. Bandung, the capital of West Java, Indonesia, is among the cities with the highest vehicle density, reaching 2.3 million registered units, and a population approaching 2.5 million residents (Badan Pusat Statistik, 2020; Indonesian National Police, 2025). This escalation in urban activity contributes to elevated concentrations of air pollutants, especially those produced by transportation, waste burning, and industrial [1].

Air pollutants are harmful substances present in the atmosphere at concentrations that pose risks to human health. Major sources include vehicle emissions, forest fires, and industrial chimneys [2]. Based on the Ambient Air Quality Standards (AAQS/GB 3095-2012), six key pollutants are used to assess air quality: particulate matter ($PM_{2.5}$ and PM_{10}), sulfur dioxide (SO_2), nitrogen dioxide (NO_2), ozone (O_3), and carbon monoxide (CO) [3]. Among these, CO is a toxic, colorless, and odorless gas produced from incomplete combustion of fossil fuels. It is flammable and dangerous, yet non-irritating, making it difficult to detect without instrumentation [4]; [5].

Exposure to CO above the permitted threshold of 25 ppm, as regulated in Indonesia's Ministerial Regulation No. 13/2012, can significantly harm human health [6]. In fact, air pollution-related mortality rates have been reported to be three times higher than those caused by malaria, tuberculosis, and AIDS combined [7]. Hence, timely and accurate air quality information is critical for public awareness and policy development [8].

While fixed monitoring stations offer reliable data, their limited spatial coverage and high installation costs restrict their effectiveness. Mobile monitoring systems offer a flexible alternative, yet many face challenges in sensor stability during motion and lack real-time data integration [9]. Therefore, it is necessary to develop low-cost, mobile, and real-time air quality monitoring solutions that can operate effectively in urban environments.

This study aims to design and implement a mobile air monitoring system based on Internet of Things (IoT) technology. The system integrates a MiCS-4514 CO gas sensor with an ESP32 microcontroller and is mounted on a bicycle to allow flexible monitoring across various urban locations. The system utilizes a smartphone to retrieve GPS data and transmit measurement results to the Antares cloud platform using MQTT protocol. Equipped with a DC pump and flowmeter, the device maintains stable airflow and ensures reliable CO readings during motion. This approach is expected to support adaptive environmental monitoring and contribute to air pollution mitigation policies, particularly within the smart city framework.

2 Method

This study employed a quantitative-experimental approach for the development and evaluation of a mobile air quality monitoring system. The methods were designed to ensure the system could operate in real-time, with reliable data acquisition, transmission, and visualization for carbon monoxide (CO) concentration monitoring. All components, procedures, and analytical processes are described in sufficient detail to allow reproducibility.

2.1 System Design Overview

The mobile air quality monitoring system was developed as a compact and efficient solution for real-time monitoring of carbon monoxide (CO) concentrations. It addresses the limitations of conventional monitoring stations in terms of spatial coverage and operational costs. By adopting an Internet of Things (IoT) approach, the system enables flexible and location-independent deployment. The system architecture integrates a microcontroller (ESP32) as the main processing unit, connected to a carbon monoxide sensor (MiCS-4514), a voltage and current sensor (INA219), a real-time clock (RTC) module, an LCD display, a MicroSD card for local data logging, and a Bluetooth module for acquiring GPS data from a smartphone. Wireless communication is established via Wi-Fi tethering to transmit data to a cloud-based IoT platform (Antares) using the MQTT protocol. This design ensures continuous environmental data acquisition and supports real-time visualization, remote access, and reliable data storage. Furthermore, the system is designed with modularity in mind, allowing for future scalability and the integration of additional sensing components.

2.2 Observation Routes and Time Schedule

The field data collection process was conducted along three designated urban traffic routes. Each route was selected based on its traffic density and environmental characteristics, such as proximity to commercial and office districts. The observations were scheduled at three different time intervals to capture the diurnal variation in pollutant concentrations corresponding to urban activity patterns.

- Rute 1: Jl. Tubagus Ismail – Jl. Sadang Serang – Jl. Cikutra – Jl. Surapati – Jl. Taman Sari
- Rute 2: Jl. Diponegoro – Jl. Supratman – Jl. Ahmad Yani – Jl. R.E. Martadinata – Jl. Ir. H. Juanda
- Rute 3: Jl. R.E. Martadinata – Jl. Sumatra – Jl. Aceh – Jl. Kalimantan – Jl. Jawa – Jl. Gudang Selatan – Jl. Ahmad Yani – Jl. Asia Afrika – Jl. Banceuy – Jl. ABC – Jl. Braga – Jl. Wastukencana.

To capture the variation in air pollutant concentrations throughout the day, observations were conducted during three distinct time intervals. These time slots were selected to reflect typical urban traffic cycles, including peak and off-peak periods. The schedule and corresponding objectives are presented in the table below.

Table 1. Observation schedule and objectives for traffic route monitoring

Route	Observation Hours	Observation Objectives
1, 2 and 3	06:00 – 10:00 WIB	Morning rush hour in office and commercial areas
1, 2 and 3	11:00 – 15:00 WIB	Afternoon traffic during lunch break and commercial activity
1, 2 and 3	15:00 – 19:00 WIB	Evening rush hour in office and commercial areas

This time-based observation structure enabled a more comprehensive analysis of pollution level fluctuations relative to human mobility patterns in urban environments.

Journal of Science and Education (JSE)
Vol 6, Issue 1, September 2025, Pages 878-890
ISSN: 2745-5351 (Media Online)
DOI: https://doi.org/10.58905/jse.v6i1.589

2.3 Block Diagram of the system

To provide a clear understanding of the system architecture, a block diagram is presented. This diagram illustrates the relationship and interaction between hardware components used in the portable CO monitoring system. The microcontroller ESP32 acts as the core of the system, managing sensor readings, data transmission, and power regulation. Each supporting module is integrated through appropriate communication protocols such as I2C, SPI, and Serial, ensuring modularity and real-time performance.

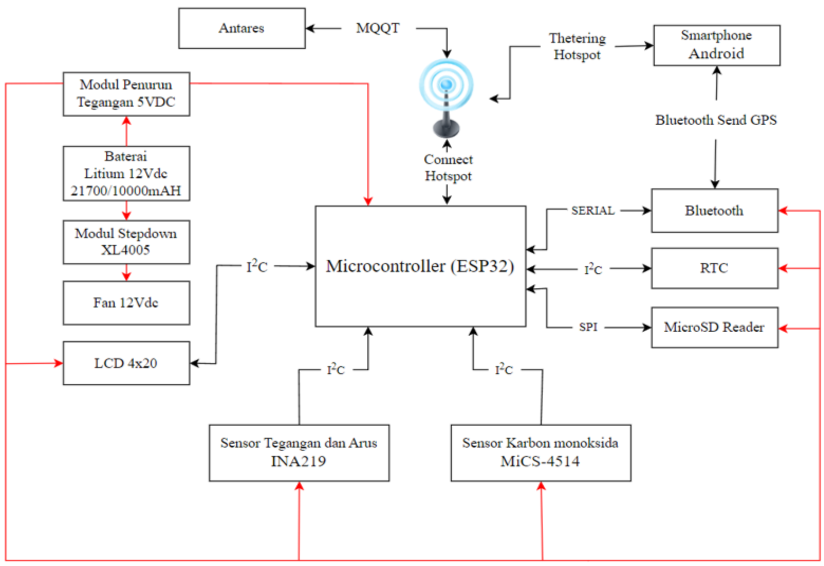

Fig. 1. Block diagram of the portable CO monitoring system based on ESP32

As shown Figure 1 in the block diagram, the system integrates various modules such as a CO sensor (MiCS 4515), voltage and current sensor (INA219), RTC, and Bluetooth, all connected to the ESP32 microcontroller. Data is stored locally via the MicroSD module and also transmitted to the Antares IoT platform through MQTT over a hotspot connection. The system is powered by a 12V lithium battery regulated through step-down converters to supply stable voltages for each module. This modular design ensures flexibility, ease of maintenance, and scalability for future sensor integration or functionality enhancements.

2.4 Design and System Architecture

To ensure accurate and stable CO gas detection in outdoor and mobile conditions, the device was designed with a protective casing that integrates all functional components into a compact structure. The mechanical layout was arranged to optimize airflow, minimize interference from ambient conditions, and facilitate real-time sensing. Figure X illustrates the physical design of the device, showing the position of critical

Journal of Science and Education (JSE)
Vol 6, Issue 1, September 2025, Pages 878-890
ISSN: 2745-5351 (Media Online)
DOI: https://doi.org/10.58905/jse.v6i1.589

components such as the inlet, outlet, CO sensor, flowmeter, microcontroller, and display interface.

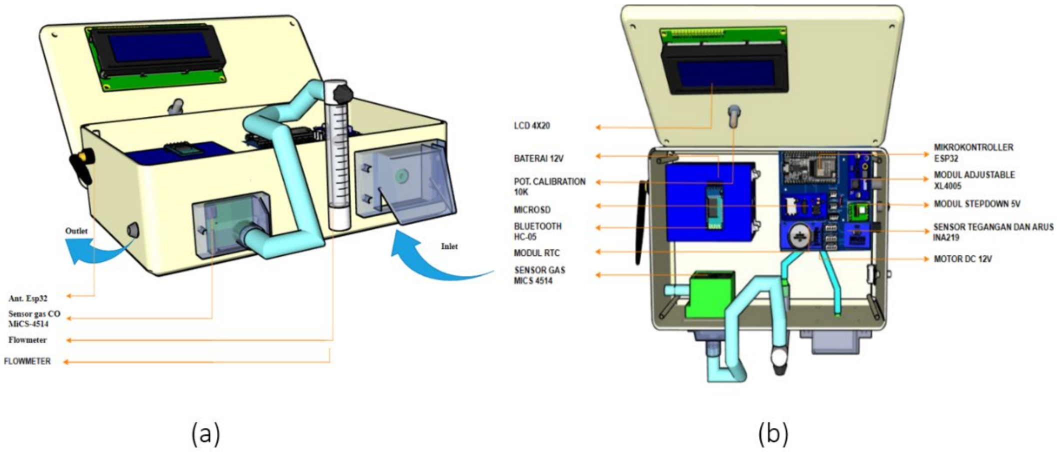

Fig. 2. Structural design of the portable CO monitoring system: (a) External front view with component labels and airflow direction; and (b) Internal layout showing electronic module integration

As illustrated in Figure 2, the portable CO monitoring device integrates a protective enclosure and modular electronics for mobile environmental sensing. The external view in Figure 2 (a) shows the inlet, outlet, flowmeter, and sensor arrangement, designed to ensure stable airflow and minimize external interference. Ambient air enters through a 3 mm inlet, is regulated by a 1 LPM flowmeter, and directed into a sealed sensor chamber (53.49 cm^3) containing the MiCS-4514 CO sensor. Air exits via a designated outlet to maintain consistent flow.

The internal layout, shown in Figure 2 (b), features an ESP32 microcontroller as the core processor. Measurement results are displayed on an LCD, logged to a microSD card, and time-stamped using an RTC. GPS data is received via Bluetooth (HC-05), and power consumption is monitored using the INA219 sensor. A DC motor, regulated by an XL4005 step-down module, ensures stable airflow. The entire system is powered by a 12V lithium battery, supporting extended mobile deployment. Figure 3 presents a flowchart detailing the operational stages, starting from device initialization to automated data acquisition and transmission.

Journal of Science and Education (JSE)
Vol 6, Issue 1, September 2025, Pages 878-890
ISSN: 2745-5351 (Media Online)
DOI: https://doi.org/10.58905/jse.v6i1.589

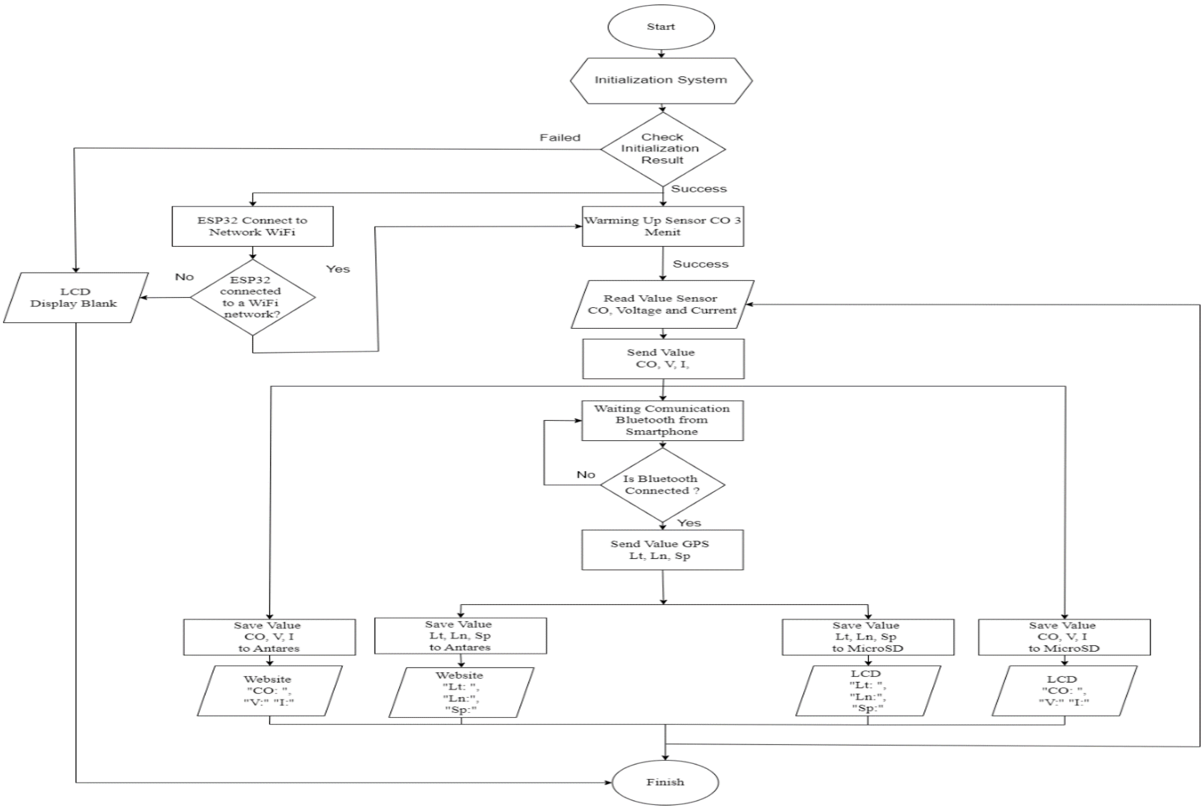

Fig. 3. Flowchart of the data acquisition and transmission process in the IoT-based

The flowchart above Figure 3 illustrates the sequential process of the IoT-based air monitoring system. The process begins with system initialization, including sensor configuration and communication module setup. Once initialization is completed, the system checks the success status. If initialization fails, the system will display an "LCD Blank" condition and halt further processes. However, if successful, the system proceeds with the warm-up phase of the carbon monoxide (CO) sensor for three minutes while simultaneously checking for Wi-Fi connectivity. If Wi-Fi is unavailable after the warm-up period, the system will terminate the process and display "LCD Blank." Conversely, if the Wi-Fi connection is successful, the system will read data from the CO sensor along with voltage and current values. The acquired data will be transmitted to the Antares platform, stored on a microSD card, and displayed on the LCD. Next, the system waits for a Bluetooth connection from the smartphone application. If the connection is not yet available, the system continues to wait. Once Bluetooth is successfully connected, GPS data including latitude (Lt), longitude (Ln), and speed (Sp) will be transmitted from the smartphone to the device and combined with the previously collected sensor data. All GPS data are then stored in both the Antares database and the microSD card, and displayed on the LCD as well as the Antares

Journal of Science and Education (JSE)
Vol 6, Issue 1, September 2025, Pages 878-890
ISSN: 2745-5351 (Media Online)
DOI: https://doi.org/10.58905/jse.v6i1.589

dashboard. After completing all processes, the system returns to the initial sensor reading phase.

2.5 Architecture of Mobile CO Monitoring System

To facilitate real-time carbon monoxide (CO) monitoring in urban environments, the system is designed as a mobile platform integrated with Internet of Things (IoT) technology. The monitoring device is mounted on a bicycle, enabling high mobility, flexible deployment, and broader spatial coverage during data collection. This configuration allows for efficient tracking of pollutant distribution across various urban routes and conditions. The system architecture, as illustrated in the following figure, comprises several key components that work in coordination to support accurate sensing, real-time data transmission, and geospatial mapping of CO concentrations.

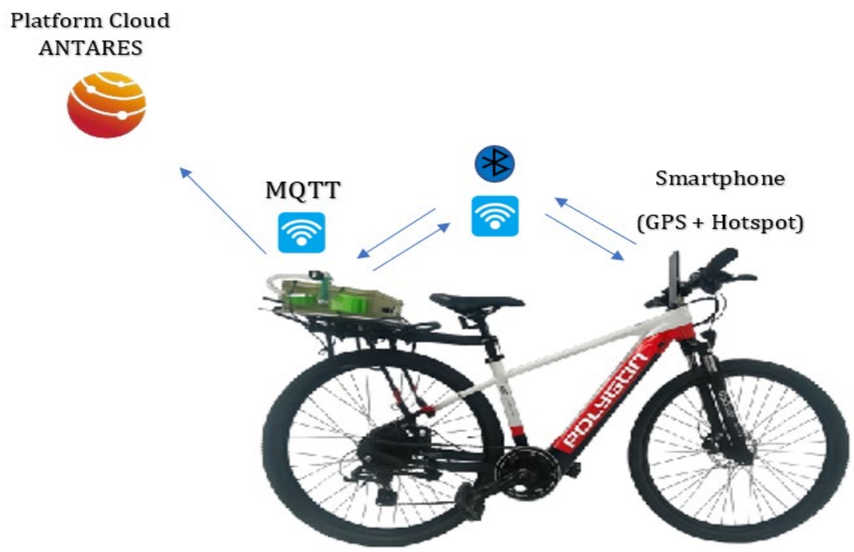

Fig. 4. Architecture of the Mobile CO Monitoring System

The figure above illustrates the data acquisition architecture of the mobile carbon monoxide (CO) monitoring system. A smartphone is utilized as a key component due to its built-in GSM and GPS capabilities, which significantly reduce system complexity and eliminate the need for additional hardware modules. The smartphone's GPS employs Assisted Global Positioning System (A-GPS) technology, which enhances positioning accuracy and responsiveness by leveraging cellular and wireless communication networks—particularly advantageous in areas with weak satellite signals, such as dense urban environments, high-rise corridors, and forested regions [10]. GPS location data—including latitude, longitude, and speed—is transmitted via Bluetooth to the HC-05 Bluetooth module embedded in the monitoring device. Additionally, the smartphone provides internet connectivity through mobile hotspot tether-

Journal of Science and Education (JSE)
Vol 6, Issue 1, September 2025, Pages 878-890
ISSN: 2745-5351 (Media Online)
DOI: https://doi.org/10.58905/jse.v6i1.589

ing, allowing the device to access the network without requiring a dedicated GSM module. The collected sensor and location data are then transmitted to the Antares cloud platform using the lightweight MQTT protocol, supporting efficient, low-power, and real-time data communication.

MQTT was selected as the communication protocol due to its lightweight and efficient architecture, making it highly suitable for resource-constrained devices commonly found in low-power Internet of Things (IoT) systems [11]. The Antares platform was chosen to facilitate real-time IoT communication and data visualization, offering user-friendly features for monitoring and analysis. One of its key advantages is the capability to export raw data in easily accessible formats such as Excel files, enhancing usability for further data processing and interpretation (Bragiwibisana et al., 2024). In addition to cloud-based storage via Antares, the system also supports local data logging through a MicroSD card. Data is saved in the .txt format, which is lightweight, human-readable, and compatible with various data processing tools such as Microsoft Excel and Python. The use of the .txt format—categorized as an open standard—ensures long-term accessibility, transparency, and interoperability across platforms [13]. This dual-storage approach enhances data reliability and supports redundancy for post-processing, analysis, and validation purposes.

2.6 Testing and Calibrations

To ensure the reliability and validity of gas concentration measurements, a comprehensive calibration process was conducted on the carbon monoxide (CO) sensor prior to field deployment. Calibration is a crucial step in the development of any sensing system, as it ensures the accuracy, consistency, and repeatability of the data collected during real-time monitoring.

Calibration Setup and Procedure.

The calibration process consisted of two standard stages: zero calibration and span calibration. Zero calibration involved the use of zero air to establish a baseline reading, while span calibration employed carbon monoxide (CO) gas at a known concentration—typically 15 ppm—to validate the sensor's responsiveness. A commonly adopted method, as demonstrated by Afshar-Mohajer et al. (2018), utilizes a sealed calibration chamber with a constant gas flow rate of 1 liter per minute (1 LPM) to ensure uniform gas exposure. In this study, calibration was performed in a controlled laboratory setting using a dedicated calibration apparatus specifically designed for gas sensor evaluation. The setup included gas flow channels and flexible tubing to connect the reference gas source to the sensor chamber. A potentiometer was used to manually adjust the sensor's sensitivity, aligning the sensor output with a reference concentration of 100.35 ppm. This procedure ensured stable and precise readings during calibration. To assess the effect of flow rate on sensor response, two flowmeters were integrated into the system, set at 0.6 LPM and 1 LPM, respectively. Each flow rate was applied for one minute, during which sensor readings were recorded at 5-second intervals. All collected data were systematically logged and averaged to determine the sensor's mean output under each condition. The subsequent analysis

Journal of Science and Education (JSE)
Vol 6, Issue 1, September 2025, Pages 878-890
ISSN: 2745-5351 (Media Online)
DOI: https://doi.org/10.58905/jse.v6i1.589

focused on signal stability, sensitivity, and response time—key parameters for evaluating the sensor's accuracy and precision under varying flow conditions.

Accuracy Calculation (%R).

The accuracy of the sensor, expressed as a percentage (%R), was evaluated to determine how closely the measured values aligned with the reference gas concentration. Accuracy was calculated using Equation (1), which represents the ratio between the mean of the measured sensor outputs and the known reference concentration. This percentage provides a quantitative assessment of the sensor's ability to deliver reliable and valid measurements during calibration.

$$\%R = \frac{\bar{x}}{\mu} . 100\ \% \tag{1}$$

Where $\bar{\mathbf{x}}$ is the mean of repeated measurements, $\boldsymbol{\mu}$ **is the true or reference value.** A result is considered accurate if the %R is within the accepted threshold, specifically ≤ 2% (Hadi et al., 2017).

Repeatability and Relative Standard Deviation (%RSD).

Repeatability, also referred to as instrument stability, is evaluated using the relative standard deviation percentage (%RSD), which quantifies the consistency of measurement results obtained under identical conditions. The %RSD is calculated using Equation (2), based on the standard deviation derived in Equation (3) and the mean of the repeated measurements obtained from Equation (4). To determine whether the observed %RSD meets the acceptable threshold for precision, a comparison is made using Equation (5). This criterion states that the measured %RSD must be less than or equal to 0.5 times the predicted %RSD, which is a function of the analyte concentration in mass fraction. If this condition is fulfilled, the measurement precision is considered acceptable and reliable (Hadi et al., 2017); [15]; & [16].

$$\%\mathbf{RSD} = \frac{\mathbf{sd}}{\bar{\mathbf{x}}} . 100\% \tag{2}$$

Where *sd* is the standard deviation and $\bar{x}$ is the mean of repeated measurements. The standard deviation is calculated as:

$$\mathbf{sd} = \sqrt{\frac{\sum_{i=1}^{n}(\mathrm{x_i} - \bar{x})^2}{\mathbf{n-1}}} \tag{3}$$

and the mean value is given by:

$$\bar{\mathbf{x}} = \frac{\sum_{i=1}^{n} X_i}{n} = \frac{X + X_2 + X_3 + \dots\dots\dots X_n}{n} \tag{4}$$

To determine whether the observed %RSD meets the acceptable precision threshold, the following criterion is applied:

$$\%\mathbf{RSD}_{\mathbf{Observasi}} \leq \mathbf{0,5\ X}\ \%\mathbf{RSD}_{\mathbf{Horwitz}} \tag{5}$$

Journal of Science and Education (JSE)
Vol 6, Issue 1, September 2025, Pages 878-890
ISSN: 2745-5351 (Media Online)
DOI: https://doi.org/10.58905/jse.v6i1.589

Where, $\mathbf{2}^{\,1-0,5log_{10}[C]}$ Horwitz Equation (predictive RSD), *sd* is standard deviation, $\bar{\mathbf{x}}$ is mean of repeated measurements, $\mathbf{C}$ is concentration of the span gas in mass fraction (100 ppm=1×10^{-4}) (Hadi et al., 2017).

3 Results and Discussion

Prior to presenting the main findings, calibration tests were carried out to ensure the accuracy and reliability of the sensor readings. This step was essential to verify the sensor's capability in detecting carbon monoxide (CO) concentrations within the expected range. The calibration results, which include measured values, reference concentrations, and error analysis, are summarized in Table 2.

Table 2. Calibration Results of CO Sensor under Different Flow Rates

Flow (LPM)	Factor Calibration	Ref. Gas (ppm)	Mean Calibrated (ppm)	Sample Size
0,6	0,26	100,35	53,00	12
1	0,27	100,35	102,7	12

The calibration results presented in Table 2 illustrate the significant influence of airflow rate on the accuracy and precision of the carbon monoxide (CO) sensor when tested with a reference gas concentration of 100.35 ppm. Two airflow conditions, 0.6 LPM and 1.0 LPM, were evaluated to determine the most reliable operating point for mobile applications. Under the 0.6 LPM condition, the average measured CO concentration was 53.01 ppm with a standard deviation of 27.73. Based on the Horwitz statistical model, the observed relative standard deviation (%RSD) was calculated at 52.32%, which substantially exceeds the acceptable threshold of 4% (equivalent to 0.5 × predicted Horwitz RSD of 8%). This high level of variation indicates poor repeatability and precision, suggesting that the sensor's response under low flow conditions is unstable and does not meet method validation criteria.

In contrast, at a flow rate of 1.0 LPM, the sensor demonstrated improved performance, with an average reading of 102.75 ppm and a significantly lower standard deviation of 1.62. The resulting %RSD was 1.58%, well below the 4% acceptance limit. These findings confirm that the sensor operates with high precision and consistency at the higher airflow rate, thereby validating its reliability for repeated measurements. Overall, the results clearly demonstrate that airflow rate plays a critical role in the performance of the CO sensor. Specifically, maintaining an optimized flow rate of 1.0 LPM enhances measurement stability and yields results closely aligned with the reference concentration, making it well-suited for mobile environmental monitoring, where consistent sampling and accurate readings are essential.

Journal of Science and Education (JSE)
Vol 6, Issue 1, September 2025, Pages 878-890
ISSN: 2745-5351 (Media Online)
DOI: https://doi.org/10.58905/jse.v6i1.589

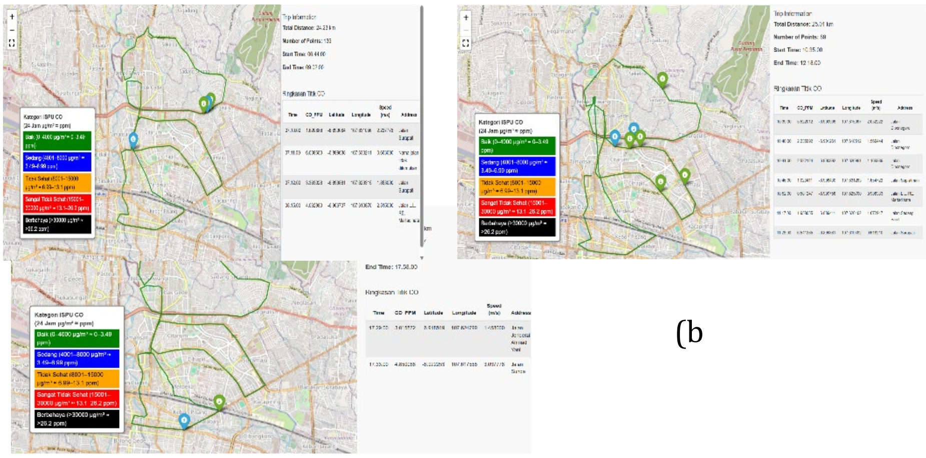

Fig. 5. CO Concentration Mapping Results during Mobile Monitoring (a) Morning Route Point Map; (b) Afternoon Route Point Map; (c) Evening Route Point Map

Table 3. Concentration Mapping Results during Mobile Monitoring

Dis. Traveled (km)	Route	Number of Point	Number Detected	Succes Rate (%)	Average CO Detected (ppm)	*SD* (ppm)
24,23	Morning	136	4	2,9	3,76	1,81
25,01	Afternoon	89	7	7,8	2,90	2,25
24,28	Evening	117	2	1,7	3,93	1,30

The results of air quality monitoring reveal varying levels of carbon monoxide (CO) concentrations across different time intervals. During the morning route (136 monitoring points), CO was detected at only 4 points, yielding a detection rate of 2.9%. The average concentration was 3.76 ppm, classified under the moderate category, with a standard deviation of 1.81 ppm. The midday route, consisting of 89 monitoring points, exhibited the highest detection rate at 7.8%. The average CO concentration during this period was 2.90 ppm, falling within the good category, with a standard deviation of 2.25 ppm. In contrast, the evening route (117 monitoring points) recorded CO presence at only 2 points (1.7%), the lowest detection rate among all intervals. However, this route showed the highest average concentration of 3.93 ppm, also categorized as moderate, with a standard deviation of 1.30 ppm.

4 Conclusion

A mobile carbon monoxide (CO) monitoring device based on the Internet of Things (IoT) has been successfully developed utilizing the MiCS-4514 sensor, an ESP32 microcontroller, and wireless communication through Bluetooth and Wi-Fi, integrated with the Antares cloud platform. The system also incorporates GPS data from a smartphone to enable spatial tracking, along with dual data storage capabilities (cloud and local). An optimized airflow design and regulation mechanism maintained a stable flow rate of 1 LPM, ensuring consistent and reliable sensor readings during mobile operation. Calibration using a 100.35 ppm CO gas reference at 1 LPM yielded a mean sensor reading of 102.7 ppm, with a standard deviation of 1.62 ppm. The resulting relative standard deviation (%RSD) was 1.58%, and the Horwitz Ratio was calculated at 0.20—both well within acceptable validation limits. Field testing across three urban routes in Bandung demonstrated the device's effectiveness in detecting CO concentrations at varying times and locations. The results showed average CO levels below 5 ppm, with standard deviations also under 5 ppm. While detection rates remained below 10%, spatial mapping revealed a clear correlation between CO concentrations and traffic density, with notably higher levels consistently recorded near major roads and intersections.

References

[1] Winatama, Derystanto, dan S. W. (2023). Analisis Kualitas Udara pada Kawasan Transportasi, Industri, Perkotaan, Permukiman, dan Perdagangan di Kota Tegal, *Jurnal Ilmu Lingkungan*, Vol. 21, No. 2, 381–386. doi:10.14710/jil.21.2.381-386

[2] Jiyal, S.; Sheetlani, J.; Saini, R. K. (2022). Internet of Things: A Survey on Air Pollution Monitoring, Challenges and Applications, *Proceedings of the 2022 7th International Conference on Computing, Communication and Security, ICCCS 2022 and 2022 4th International Conference on Big Data and Computational Intelligence, ICBDCI 2022*, 1–6. doi:10.1109/ICCCS55188.2022.10079635

[3] Wang, J.; Zhao, Y.; Xu, M. (2022). Distribution Characteristics of Six Criteria Air Pollutants Under Different Air Quality Levels in Cangzhou City, China, *Journal of Health and Environmental Research*, Vol. 8, No. 1, 9. doi:10.11648/j.jher.20220801.12

[4] Rambing, V. V; Umboh, J. M. L.; Warouw, F. (2022). Literature Review: Gambaran Risiko Kesehatan pada Masyarakat akibat Paparan Gas Karbon Monoksida (CO), *Kesmas*, Vol. 11, No. 4, 95–101

[5] Fairuz Rofifah Arifin; Nazwa Aulia Rahman. (2024). Analisis Pengaruh Emisi Zat Karbon terhadap Kerusakan Kualitas Udara dan Pencemaran Lingkungan, *Journal Innovation In Education*, Vol. 2, No. 1, 278–287. doi:10.59841/inoved.v2i1.1043

[6] Ruviana, R.; Setyawan, A.; Musniati, N. (2022). Relationship of Exposure to Carbon Monoxide and other factors with Blood Pressure of Motorcycle Workshop Workers in Pancoran Mas Subdistrict, Depok City, *Jurnal Keselamatan Kesehatan Kerja Dan Lingkungan*, Vol. 3, No. 1, 45–51. doi:10.25077/jk3l.3.1.45-51.2022

[7] Rizaldi, M. A.; Azizah, R.; Latif, M. T.; Sulistyorini, L.; Salindra, B. P. (2022). Literature Review: Dampak Paparan Gas Karbon Monoksida Terhadap Kesehatan Masyarakat yang Rentan dan Berisiko Tinggi, *Jurnal Kesehatan Lingkungan Indonesia*, Vol. 21, No. 3, 253–265. doi:10.14710/jkli.21.3.253-265

[8] Din, D.; Hasanuddin, Z. B.; Panggalo, S. (2024). Rancang Bangun Sistem Pemantauan Kualitas Udara Berbasis Internet of Things (IoT) Menggunakan Thingspeak dan Website, *Jurnal EKSITASI*, Vol. 3, No. 1, 17–22

[9] Shevchenko, D. V.; Holub, B. L. (2025). Regression analysis as a tool for identifying patterns in atmospheric air monitoring data, *CEUR Workshop Proceedings*, Vol. 3943, 20–27

[10] Feng, S.; Law, C. L. (2002). Assisted GPS and its impact on navigation intelligent transportation systems, *IEEE Conference on Intelligent Transportation Systems, Proceedings, ITSC*, Vols 2002-January, No. September, 926–931. doi:10.1109/ITSC.2002.1041344

[11] Mus Mulyadi Usman. (2020). Rancang Bangun Aplikasi MonitoringKetinggian Air Sungai Berbasis Internet ofThings Menggunakan Amazon Web Service, *Jurnal Teknik Elektro Dan Komputer*, Vol. 9, No. 2, 73–80

[12] Bragiwibisana, B.; Fikra Titan, F. T. S.; Permatasari, I. (2025). Pengiriman Data Sensor Untuk Deteksi Logam Yang Bersifat Metal Dengan Menggunakan Platform Antares, *Jurnal SINTA: Sistem Informasi Dan Teknologi Komputasi*, Vol. 1, No. 4, 191–199. doi:10.61124/sinta.v1i4.31

[13] Hart, E. M.; Barmby, P.; LeBauer, D.; Michonneau, F.; Mount, S.; Mulrooney, P.; Poisot, T.; Woo, K. H.; Zimmerman, N. B.; Hollister, J. W. (2016). Ten Simple Rules for Digital Data Storage, *PLoS Computational Biology*, Vol. 12, No. 10, 1–12. doi:10.1371/journal.pcbi.1005097

[14] Hadi, A.; Ahmad Subarja, J. A. S.; Firdaus, I. F. (2017). Validasi Metode Kalibrasi Gas Analyzer Untuk Pengukuran O2, Co, No, No2, So2, Ch4, Dan H2S Secara Perbandingan Langsung Dengan Ceritified Span Gas, *Jurnal Ecolab*, Vol. 11, No. 2, 62–71. doi:10.20886/jklh.2017.11.2.62-71

[15] Pitalokasari, O. D.; Fiqri, S.; Ayudia, D. (2021). Validasi Metode Pengujian Biochemical Oxygen Demand (BOD) Dalam Air Laut Secara Titrimetri Berdasarkan SNI 6989.72:2009, *Ecolab*, Vol. 15, No. 1, 63–75. doi:10.20886/jklh.2021.15.1.63-75

[16] Horwitz, W.; Albert, R. (2006). The Horwitz ratio (HorRat): A useful index of method performance with respect to precision, *Journal of AOAC International*, Vol. 89, No. 4, 1095–1109. doi:10.1093/jaoac/89.4.1095

